Научном већу Института за физику Београд

Београд, 5. јул 2013.

Предмет:
Молба за покретање поступка за стицање звања истраживач сарадник

С обзиром да испуњавам критеријуме прописане од стране Министарства просвете, науке и технолошког развоја за стицање звања истраживач сарадник, молим Научно веће Института за физику Београд да покрене поступак за мој избор у наведено звање.

У прилогу достављам:

1. Мишљење руководиоца пројекта
2. Кратку биографију
3. Списак објављених радова и њихове копије
4. Потврду о упису на докторске студије
5. Потврде о завршеним основним и мастер студијама

Са поштовањем,

Марко Младеновић

Научном већу Института за физику Београд

Београд, 5. јул 2013.

Предмет:
Мишљење руководиоца пројекта за избор Марка Младеновића у звање истраживач сарадник

Колега Марко Младеновић је запослен у Лабораторији за примену рачунара у науци Института за физику Београд од 1. новембра 2012. године. Он је ангажован на пројекту основних истраживања Министарства за просвету, науку и технолошки развој ОН171017 под називом "Моделирање и нумеричке симулације сложених вишечестичних система". С обзиром да испуњава критеријуме прописане од стране Министарства просвете, науке и технолошког развоја, сагласан сам са покретањем поступка за избор Марка Младеновића у звање истраживач сарадник.

За састав Комисије за избор Марка Младеновића у звање истраживач сарадник предлажем колеге:

(1) др Ненад Вукмировић, виши научник сарадник, Институт за физику Београд,
(2) др Игор Станковић, научник сарадник, Институт за физику Београд,
(3) др Петар Матавуљ, ванредни професор Електротехничког факултета
    Универзитета у Београду.

Руководилац пројекта,

др Александар Белић,
научни саветник, Институт за физику Београд

Biografija Marka Mladenovića

Marko Mladenović je rođen 2.9.1988 u Zaječaru. Završio je Matematičku gimaziju u Beogradu kao nosilac Vukove diplome. Potom upisuje Elektrotehnički fakultet u Beogradu, odsek fizička elektronika, smer nanoelektronika, optoelektronika i laserska tehnika. Fakultet je završio sa prosečnom ocenom 9.78 kao najbolji student generacije na odseku. Zatim upisuje master studije na istom fakultetu na modulu nanoelektonika i fotonika. Master rad pod nazivom "Atomska i elektronska struktura granica između kristalnih domena u naftalenu" je odbranio 17. 9. 2012. Doktorske studije na istom fakultetu i modulu upisuje 30.11.2012.

Kandidat je započeo svoj istraživački rad na Institutu za fiziku u Beogradu u Laboratoriji za primenu računara u nauci 2. 8. 2011, a zaposlen je od 1. 11. 2012. Angažovan je na projektu Ministarstva prosvete, nauke i tehnološkog razvoja Republike Srbije ON171017 "Modeliranje i numeričke simulacije složenih višečestičnih sistema", kao i na FP7 projektu Evropske komisije "Elektronski trasnport u organskim materijalima". Do sada je učestvovao na većem broju međunarodnih konferencija i škola. Objavio je jedan rad M21 kategorije, ima jedan rad M22 kategorije prihvaćen za objavljivanje i jedan objavljen rad M24 kategorije.

Marko Mladenović - Spisak publikacija i saopštenja sa konferencija:

M21

1) Marko Lj. Mladenovic, Nenad Vukmirovic and Igor Stankovic, "Electronic States at Low-angle Grain Boundaries in Polycrystalline Naphthalene" *J. Phys. Chem. C*, DOI: 10.1021/jp404825h

M22

2) Marko Lj. Mladenovic, Nenad Vukmirovic and Igor Stankovic, "Atomic and electronic structure of grain boundaries in crystalline organic semiconductors" *Phys. Scr. T*, prihvacen za objavljivanje

M24

3) M. Mladenovic and I. E. Stankovic, "Monte Carlo Simulations of Crystalline Organic Semiconductors" *Serbian journal of electrical engineering* **10,** 125-134 (2013), DOI: 10.2298/SJEE1301125M

M34

4) M. Mladenovic, I. E. Stankovic and N. Vukmirovic, "Atomic and electronic structure of grain boundaries in crystalline organic semiconductors" *Book of Abstracts, 3rd International conference on optical materials, 3-6 September 2012, Belgrade, Serbia, p. 90*

5) M. Mladenovic, N. Vukmirovic, I. Stankovic, "Simulations of electronic states in polycrystalline naphthalene" *DPG 2013 Conference, 10-15 March 2013, Regensburg, Germany, Poster HL 69.12*

M63

6) M. Mladenovic and I. E. Stankovic, "Monte Karlo simulacije kristalnih organskih poluprovodnika" *56th ETRAN* (2012), *Zlatibor, Serbia*

Article

Electronic States at Low-Angle Grain Boundaries in Polycrystalline Naphthalene

Marko Ljubisa Mladenovic, Nenad Vukmirovic, and Igor Stankovic

Just Accepted

Electronic States at Low-angle Grain Boundaries in Polycrystalline Naphthalene

Marko Mladenović,[*] Nenad Vukmirović, and Igor Stanković

Scientific Computing Laboratory, Institute of Physics Belgrade, University of Belgrade,

Pregrevica 118, 11080 Belgrade, Serbia

E-mail: marko.mladenovic@ipb.ac.rs

[*]To whom correspondence should be addressed

1

Abstract

We investigated the influence of grain boundaries on electronic properties of polycrystalline organic semiconductor naphthalene. Atomic structure of grain boundaries was found using a Monte Carlo method, while electronic structure calculations were performed using the charge patching method. We found that grain boundaries introduce trap states within the band gap of the material. Our results show that spatial positions and energies of trap states can be predicted solely from geometrical arrangement of molecules near the boundary. Wave functions of these states are localized on closely spaced pairs of molecules from opposite sides of the boundary. The energies of trap states are strongly correlated with the distances between the molecules in the pair. These findings were used to calculate the electronic density of trap states, which was found to exhibit a qualitatively different behavior for grain boundaries perpendicular to the *a* and *b* direction of the crystal unit cell.

2

Introduction

Organic semiconductors are materials of great promise for electronic devices, such as organic field-effect transistors (FET), organic light emitting diodes (LED) and organic solar cells (OSC).[1–7] Their advantage over inorganic counterparts is that they are flexible and have low processing cost. However, devices made of organic semiconductors still have relatively low charge mobility and low efficiency. Small molecule based crystalline organic semiconductors (such as tetracene, pentacene, rubrene, etc.) exhibit the highest mobilities among organic semiconductors due to their crystalline structures. Electronic devices based on these materials are typically obtained using vacuum-evaporation technique.[8–13] More recently, it became possible to use an inexpensive solution processing technique to obtain structures with high degree of crystallinity and good charge transport properties,[14–19] which opens the way towards large scale applications of small molecule based organic semiconductors. Therefore, researchers put effort to improve properties of these materials in order to make them competitive with inorganic semiconductors.

Thin films of crystalline organic semiconductors have a polycrystalline form, which is composed of many different crystalline grains. It has been shown that the transport in a single grain boundary device is limited by the grain boundary.[9] A pronounced dependence of transistor characteristics on the grain size was also established,[12,15,16,20] as well as a strong difference between the characteristics of single crystal and polycrystalline transistors based on the same material.[11] It was also shown that grain boundary orientation has a large influence on the charge carrier mobility.[18] All these results indicate that grain boundaries are the most limiting intrinsic factor for efficient charge transport in small molecule based polycrystalline organic semiconductors.

However, there is still a lack of understanding of the specific mechanism by which grain boundaries affect the charge transport. It is typically assumed that they introduce trap states localized at the grain boundary, with energies of these states within the band gap of the material.[9,11,12,20–22] The charges in the trap states do not contribute to transport and therefore the presence of traps reduces the effective charge carrier mobility. On the other hand, there are some suggestions that grain boundaries act as barriers and that charge carriers are trapped in the grains.[23,24] Calculations

of electrostatic potential at molecules near the grain boundary formed from two misaligned grains indicate the presence of trapping centers at the boundary.[25] Other theoretical and computational studies are primarily focused on the properties of single crystals.[26–37]

In this paper we shed light on the nature of electronic states at grain boundaries in organic crystalline semiconductors. We directly calculate the wave functions of electronic states and gain microscopic insight into the origin of these states. Using these insights, we develop a simple model for density of trap states prediction. In the following section, the method for electronic structure calculation is introduced. We use naphthalene as a representative of crystalline organic semiconductors based on small molecules. The results of the calculation of electronic states at grain boundaries are presented. We find that grain boundaries produce trap states in the band gap, where the highest states are localized on pairs of molecules at the grain boundary, whose mutual distance is much smaller than the corresponding distance in the monocrystal. Strong correlation between the mutual distance between these molecules and the energies of these states was found. Such a correlation enables one to calculate the electronic density of states at the grain boundary directly from mutual distances between molecules. Finally, the results obtained are discussed with a particular focus on their relation to the current body of knowledge about grain boundaries in organic polycrystals.

Method for electronic structure calculations

The method used for electronic structure calculations of grain boundaries in polycrystalline naphthalene is schematically described in Figure 1. The atomic structure is obtained from a relaxation procedure based on a Monte Carlo (MC) method,[38] and is subsequently used to calculate the electronic states using the density functional theory (DFT)[39] based charge patching method (CPM).[40,41]

Initial configuration for MC relaxation are two monocrystals with different crystalline orientations joined at their common boundary. Potential energy of a system is calculated using Transfer-
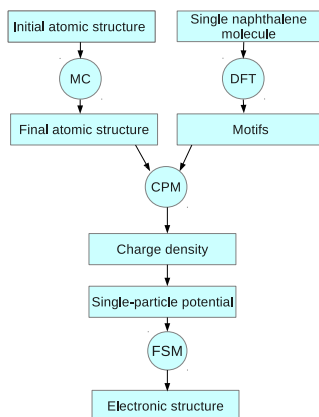
4

Figure 1: Schematic representation of the algorithm for electronic structure calculations.

able potentials for phase equilibria (TraPPE).[42,43] Naphthalene molecules are considered as rigid bodies, hence only interactions between carbon atoms from different molecules described by the weak Van der Waals interaction are taken into account. Carbon - hydrogen (CH) groups are treated as one atom with a center of mass at carbon atoms. TraPPE parameters for interactions between CH groups are: $\sigma = 3.695$ Å, $\varepsilon/k_B = 50.5$ K and for interaction between C atoms: $\sigma = 3.7$ Å, $\varepsilon/k_B = 30$ K. A MC algorithm was then used to minimize the energy of the system. In each step of the MC algorithm, one molecule is randomly chosen, translated for a randomly chosen vector and rotated by a randomly chosen angle. The decision about the acceptance of this move is made according to the Metropolis algorithm: if the energy of the new configuration is lower than the initial, the move is accepted; otherwise, it is accepted with a probability equal to the Boltzmann weight of the difference of the energy of the new and the old configuration.[38] The simulation is performed until a thermal equilibrium is reached, which is evidenced by the saturation in the dependence of the energy on the number of simulation steps. Simulation is performed at a temperature of 300 K. After the thermal equilibrium is reached, the system is gradually cooled down to 0 K. In this way, dynamic disorder (crystal disorder induced by thermal motion) effects[26] are excluded. Both the effects of dynamic disorder and grain boundaries can in principle induce localized states and it would be very difficult to distinguish between these if the electronic structure calculations

5

were performed for a structure obtained from a snapshot of MC simulations at 300 K. To check that the choice of the temperature of 300 K has only a small effect on the final atomic structure obtained from a MC procedure, we repeated the simulations using the temperatures of 100 K, 200 K and 400 K, as well. Atomic structures obtained from these simulations were nearly identical as the atomic structure obtained from the simulation at 300 K. Therefore, MC simulation procedure is robust in the sense that the final structure is weakly dependent on the details of the procedure.

TraPPE empirical potentials were previously used for variety of organic materials.[43–45] The validity of the potentials used in the MC simulation was verified by comparing the naphthalene crystal lattice constants obtained from these empirical potentials to the values from the literature. Initial structure for the crystal lattice parameters optimization is the naphthalene unit cell with lattice parameters and atomic structure given in Ref. 46. It is assumed that two angles of the unit cell are $90°$, since the naphthalene unit cell is monoclinic.[47] Other unit cell parameters (3 lengths and one angle) were varied and MC relaxation was performed for each combination of the unit cell parameters until the convergence of the potential energy was satisfied. In the same manner as for the atomic structure of grain boundaries, the simulation was firstly performed at 300 K, followed by gradually cooling down to 0 K. The obtained lattice constants are constants which give the crystal lattice with minimal potential energy: $a = 8.325$ Å, $b = 5.92$ Å, $c = 7.77$ Å and $\beta = 63°$. In the literature there are several results for naphthalene unit cell parameters: in Ref. 48 $a = 8.4$ Å, $b = 6$ Å, $c = 8.66$ Å and $\beta = 57.1°$; in Ref. 49 $a = 8.098$ Å, $b = 5.953$ Å, $c = 8.652$ Å and $\beta = 55.6°$. Therefore, lattice constants obtained with TraPPE empirical potentials are in good agreement with previous results. Simulations were performed using temperatures other than 300 K, as well, to check the correctness of the procedure and the results. For additional evaluation of the validity of empirical potentials, the melting temperature of naphthalene was calculated as the temperature of the heat capacity peak.[50] The calculated melting temperature is 340 ± 5 K, which is close to the melting temperature of 352.5 K given in Ref. 51.

After the atomic structure is obtained, electronic structure calculations can be performed. In principle, DFT can be used for that. However, to avoid finite size effects on the electronic states at

6

the grain boundaries, one needs to include a sufficiently large number of unit cells in the plane of the boundary, as well as several molecular layers nearest to the boundary. This typically includes several thousand atoms, which is beyond the reach of standard DFT calculations. Therefore, the CPM was used instead of standard DFT. CPM is a strong tool by which one can directly construct the electronic charge density instead of self-consistently solving the Kohn-Sham equations as in standard calculations based on DFT. In the CPM, an appropriate motif is assigned to each atom in the system. Motif is a description of the environment of an atom. It contains the information about the types of the central atom and its neighbors. There are 5 motifs in the system that consists of naphthalene molecules only: $C_3 - C_3C_2C_2$, $C_2 - C_3C_2H$, $C_2 - C_2C_2H$, $H - C_2 - C_2C_2$, $H - C_2 - C_3C_2$, where C_X is the carbon atom connected to X other carbon atoms. Charge density of a motif associated to an atom A is calculated using the formula:

$$m_A(r - R_A) = \frac{w_A(r - R_A)}{\sum_B w_B(r - R_B)} \rho(r),$$ (1)

where $\rho(r)$ is the charge density of a single naphthalene molecule obtained by DFT calculations, while R_A and w_A are respectively the position and the weight function of the atom A. Overall charge density is then calculated as a sum of all motif charge densities in the system. With charge density at hand, the single-particle Hamiltonian is given as:

$$H = -\frac{\hbar^2}{2m_0}\nabla^2 + v_I + \frac{e}{4\pi\varepsilon_0}\int \frac{\rho(r')}{|r - r'|}dr' + v_{xc}^{LDA}(\rho).$$ (2)

The first term in Eq. (2) is the kinetic energy, the second term is the atomic core pseudopotential modeled using norm-conserving pseudopotentials, the third term is the electrostatic Hartree potential, while the fourth term is the exchange-correlation term, which is modeled using the local density approximation (LDA). The eigenvalue problem of the Hamiltionian is solved using the folded spectrum method (FSM),[52] as implemented in the PESCAN code that gives the electronic states around the desired energy, which is the top of the valence band in our case.
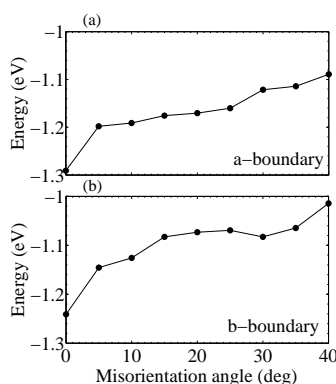
7

Wave functions at grain boundaries

Figure 2: The dependence of potential energy of the system per molecule on the misorientation angle between monocrystal grains for *a*-boundary systems (a) and *b*-boundary systems (b). Each system consists of 1000 molecules.

In this section the wave functions of states at grain boundaries are presented. We consider the system consisting of 1000 molecules (500 at each side of the boundary) arranged in 10 layers which are parallel to the *ab* plane[47] of the unit cell. Electronic structure calculations are performed for a single layer of molecules, which is sufficient to describe the electronic properties of the material, because the electronic coupling in the *c* direction is much weaker than in the *ab* plane. Calculations are performed for several misorientation angles between the grains: $5°$, $10°$, $15°$ and $20°$ and for 2 types of grain boundaries: (1) perpendicular to the *a* direction (*a*-boundary) and (2) perpendicular to the *b* direction (*b*-boundary) of the unit cell. Only small angles are considered, because total energy of the system increases as the angle of misorientation increases, as demonstrated in Figure 2. For each system, the energies of the 10 highest occupied states in the valence band and their wave functions are calculated.

Results of electronic structure calculations for the *a*-boundary system with misorientation angle of $10°$ are presented in Figure 3. These results indicate that there are several states in the band gap which energies are significantly higher than the energies of the other states. These states are trap states for charge carriers and could strongly affect transport properties of the material. Wave functions of the first and the second highest occupied state are localized on the two molecules
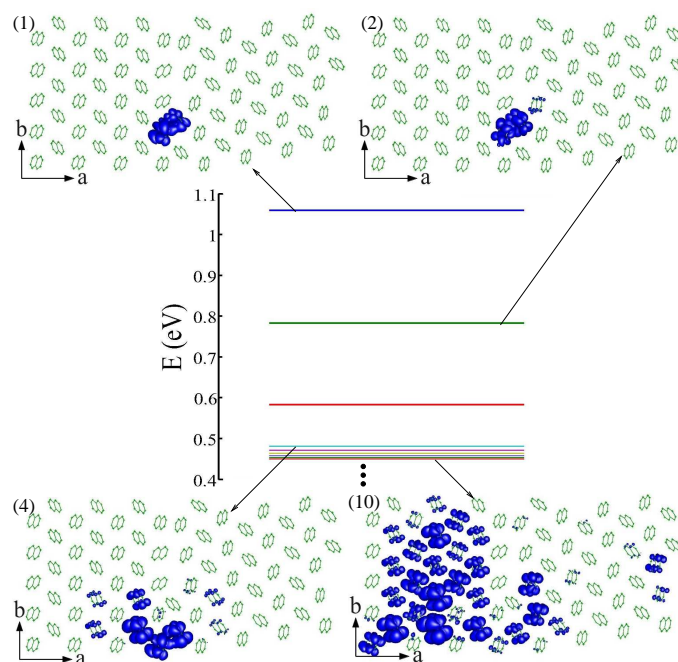
8

Figure 3: Energies of the states at the top of the valence band and the isosurfaces of their wave function moduli for the system with the misorientation angle of 10° and the grain boundary perpendicular to the *a* direction. Isosurfaces correspond to the probability of finding a hole inside the surface of 90%.

9

at the grain boundary. Distance between these two molecules (defined hereafter as the distance between their centers of mass) is 3.45 Å, while the distance between two nearest molecules in the monocrystal is about 5 Å. Highest occupied states in organic semiconductors originate from electronic coupling of HOMO (highest occupied molecular orbital) levels of different molecules. Electronic coupling that results from the overlap of HOMO orbitals is strongest for closely spaced molecules. As a consequence, the highest state in Figure 3 is localized on two molecules with smallest mutual distance. It is the bonding states of HOMO orbitals of the two molecules, while the second state in Figure 3 is the antibonding state. At certain energies the spectrum becomes nearly continuous and the states which are completely delocalized start to appear, such as the 10th calculated state, see Figure 3. States like this originate from delocalized Bloch states of the monocrystal and therefore are not induced by grain boundaries.

Electronic calculations for other misorientation angles and boundary directions show similar results. In Figure 4, the results for *b*-boundary system and misorientation angle of $10°$ are presented. In this case, there is only one molecule pair at the grain boundary with small mutual distance and consequently one trap state deep in the band gap. Other states are delocalized.

The presented results indicate that grain boundaries introduce electronic states within the band gap of the material. Hereafter, the states localized at the boundaries will be called trap states, while delocalized states will be called valence band states. Some trap states are very deep in the band gap, even more than 1 eV above the valence band. As a reference, experimentally measured band gap of naphthalene is about 5.2 eV.[48] The traps with energies significantly above the top of the valence band (more than 0.1 eV) are always localized on two molecules belonging to different grains with mutual distance less than the distance between two nearest molecules in the monocrystal. Such pairs of molecules will be hereafter called trapping pairs. Other localized states at the grain boundary have energies very close to the energies of the top of the valence band (second state in Figure 4, for example). Consequently, only pairs of molecules (trapping pairs) will be taken into account. We find that there is a strong correlation between the distance between the molecules in trapping pairs and the energy of the trap electronic states. This dependence is shown in Figure
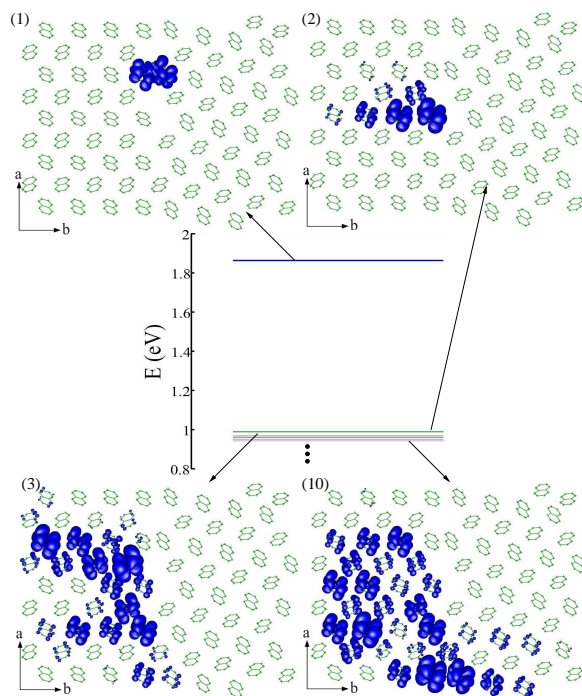
10

Figure 4: Energies of the states at the top of the valence band and the isosurfaces of their wave function moduli for the system with the misorientation angle of $10°$ and the grain boundary perpendicular to the b direction. Isosurfaces correspond to the probability of finding a hole inside the surface of 90%.

5. The best fit of this dependence is given by an exponential function $\Delta E = Ae^{B(R-R_0)}$, where $A = 1.4064\,\text{eV}$, $B = -4.181\,\text{Å}^{-1}$ and $R_0 = 3.2\,\text{Å}$.
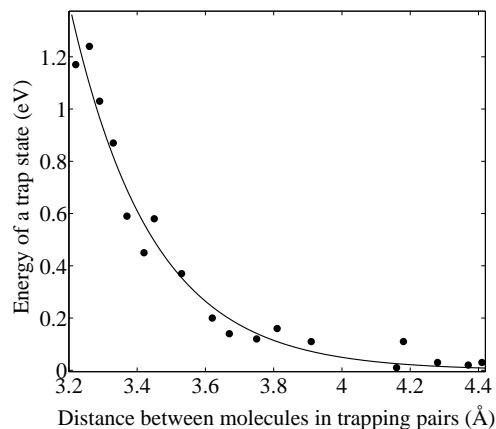

Figure 5: The dependence of the energy of the grain boundary induces trap states on the distance between molecules in trapping pairs. The data obtained from all simulated systems are presented in the figure. Energies of the trapping states are defined with the top of the valence band as a reference level.

Density of trap states at grain boundaries

Electronic structure calculations can be performed for relatively small boundaries only. While such calculations were highly valuable for understanding the origin and the degree of wave function localization at the boundary, they do not provide sufficient statistics to reliably calculate the density of trap states. On the other hand, the remarkable dependence, presented in Figure 5 can be used to predict the energy of a trap at a given boundary without any electronic calculation, solely based on the distances between the molecules. This allows us to calculate the energies of all trap states for very large grain boundaries and consequently calculate the electronic density of trap states. Based on the degree of scattering of the data from the fit in Figure 5, we estimate that this method produces an error in the trap energy calculation of up to $0.1\,\text{eV}$.

Consequently, we have demonstrated that computationally demanding electronic structure calculations can be avoided using the aforementioned approach. Next, we show that even the MC

12

relaxation step can be avoided without significantly compromising the accuracy of electronic density of trap states. By inspecting the atomic structure near the boundaries in Figure 3, one can notice that it stays nearly unchanged after the relaxation. Only molecules in the vicinity of the boundary slightly change their positions and orientations. The difference in the distance between two molecules in trapping pairs, before and after the relaxation is below 0.1 Å, as demonstrated in Figure 6. Consequently, both MC relaxation and electronic structure calculations can be avoided in the calculation of electronic density of trap states.
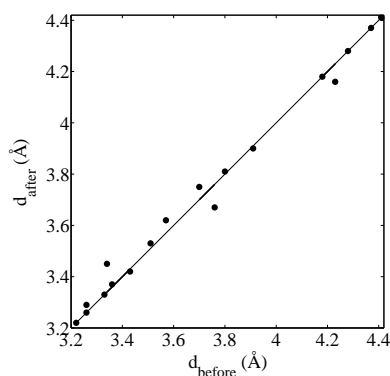

Figure 6: Dependence of the distance between trapping molecule pairs after MC relaxation (d_{after}) on the distance between them before MC relaxation (d_{before}).

The electronic density of trap states was extracted from the calculations of grain boundaries that contain 100 000 molecules arranged in 100 layers. In the construction of grain boundary atomic structure, there is an ambiguity related to the width of the void between the two monocrystals that form the boundary. This issue was overcome by shifting one of the crystals in the direction perpendicular to the boundary and selecting the void width in such a way that the potential energy of the system is minimal.The distribution of distances between trapping pairs of molecules is calculated then. Next, using the previously introduced exponential fitting function, the electronic density of trap states is obtained. The results are presented for 4 different angles: $5°$, $10°$, $15°$ and $20°$ and for 2 orientations of grain boundaries: *a*-boundary and *b*-boundary. As can be seen from Figure 5, trapping pairs with mutual distances below 4 Å are responsible for traps which are deep in the band gap. Other trapping pairs produce shallow traps which are close to the top of the valence

13

band. The distribution of distances between molecules in trapping pairs at the grain boundaries is shown in Figure 7. One should note that molecule pairs with distances below 3.2 Å can also exist. However, these were not present in small systems calculated in the previous section, hence their energy can not be reliably calculated using the fitting function. Nevertheless, such states are rather rare and we neglect their surface density.
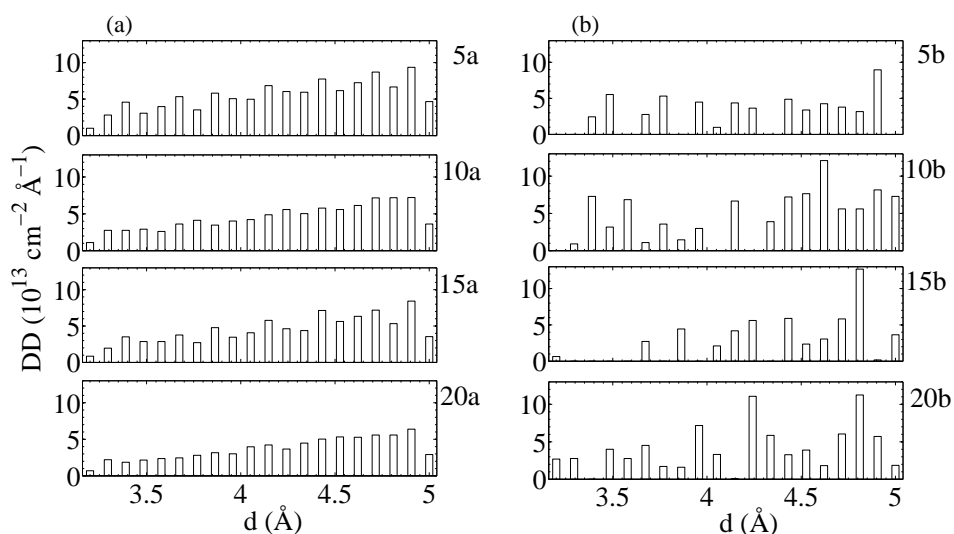

Figure 7: Trapping pair distance (*d*) distributions (DD) at different grain boundaries. The boundaries are denoted as *Xy*, where *X* is the angle between monocrystal grains and *y* is the direction perpendicular to the boundary surface.

By inspecting Figure 7, one can notice that trapping pairs distance distributions for *a*-boundary systems are similar for all angles. All of them are increasing functions with similar shapes. On the other hand, the distributions for *b*-boundary systems largely depend on misorientation angle. In addition, the distribution is not continuous as it is for *a*-boundary and some distances are preferred. This difference can be explained by the geometry of the naphthalene unit cell. Only *a* and *c* directions of the unit cell are not perpendicular. Therefore, the *c* direction is not parallel to the *a*-boundary surface. For this reason, in the case of *a*-boundary, different *ab* planes give different contribution to trapping pair distance distribution. By adding the contribution from different *ab* planes, one obtains a continuous function. In the case of *b*-boundary, *c* direction is parallel to the

14

grain boundary surface. Consequently, molecule pairs from one *ab* plane have their copies in other *ab* planes and each *ab* plane gives the same contribution to trapping pair densities. This produces discrete trapping pair distance distributions. Difference between *a*- and *b*-boundary is illustrated in Figure 8, where spatial distribution of trapping pair distance is given. Each filled circle in Figure 8 represents a molecule in the layer at the grain boundary. The color of the circle indicates the distance between that molecule and the nearest molecule from the opposite side of the boundary. As one can notice, in the case of *a*-boundary, distributions for different *ab* planes are different (as evidenced by the non-periodicity of the pattern shown in Figure 8a), while distributions for different *ab* planes in the case of *b*-boundary are equal (as evidenced by the periodic pattern in Figure 8b).
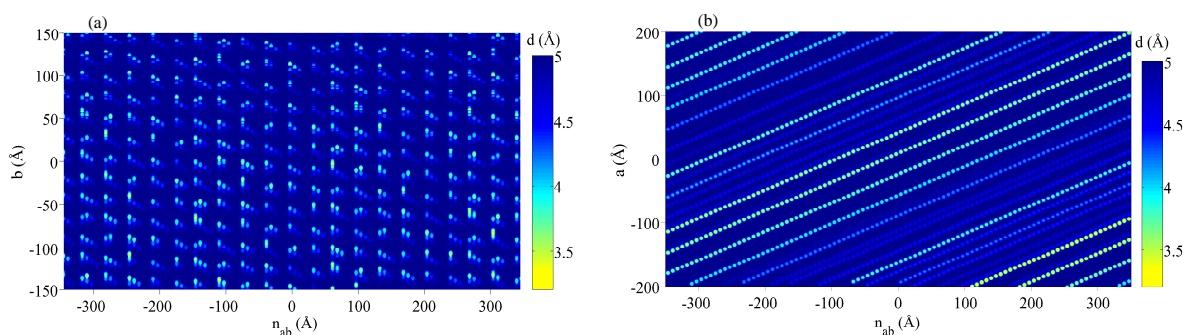

Figure 8: Spatial trapping pair distance distribution for *a*-boundary (a) and *b*-boundary (b) system with the misorientation angle of $10°$. Axis perpendicular to the *ab* plane is denoted as n_{ab}. Spatial trapping pair distance distribution is calculated using radially symmetric weight function[53] calculated at position of molecular center of mass with cut-off radius of 14.8 Å.

With trapping pairs distance distributions at hand, the electronic density of trap states can be straightforwardly calculated as explained. Densities of trap states for 8 aforementioned boundaries are given in Figure 9. Since the focus of this work is on trap states that are significantly above the top of the valence band, only trapping pairs with mutual distances below 4 Å are included in the distribution shown in Figure 9. In addition, we have assumed that each trapping pair introduce one trap states, although in some cases it can introduce two trap states, as demonstrated in Figure 3. For *a*-boundary systems, density of trap states weakly depends on angle. Going deeper in the band gap, density of trap states monotonously decreases which is a consequence of the monotonously

15

decreasing density of trapping pairs at the grain boundary. For *b*-boundaries, density of trap states

is discrete with some distances preferred as a consequence of discrete density of trapping pairs at
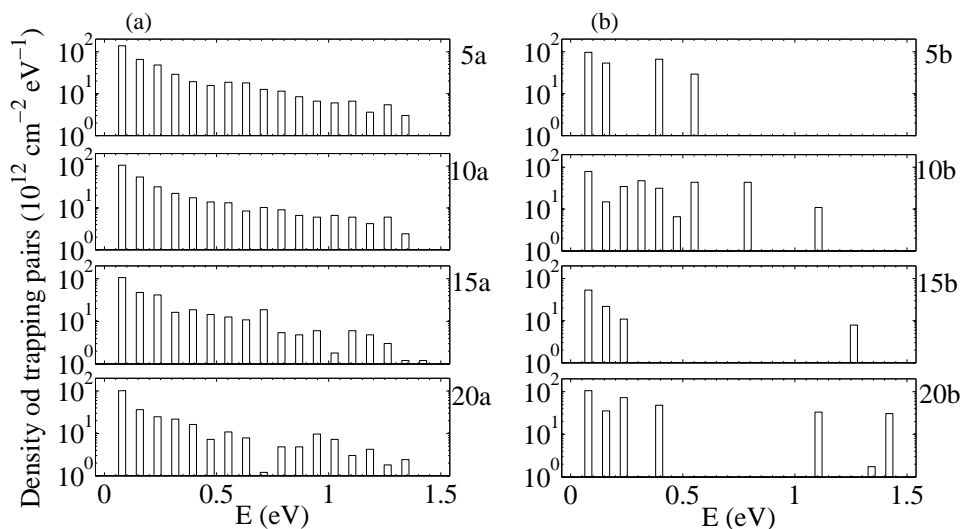
the grain boundary.

Figure 9: Electronic density of trap states at different grain boundaries. The boundaries are denoted as *Xy*, where *X* is the angle between monocrystal grains and *y* is the direction perpendicular to the boundary surface. Densities of trap states are given in a logarithmic scale. Energies of the trapping states are defined with the top of the valence band as a reference level.

Discussion

Our results clearly demonstrate the presence of trap states at the positions in the grain bound-

ary where two molecules from opposite sides of the boundary are closely spaced and hence the

electronic coupling of their HOMO orbitals is rather strong. In Ref. 23 it was argued that grain

boundaries act as barriers for charge carriers rather than traps. Such an argument was drawn from

an assumption that electronic coupling between molecules is weaker at the grain boundary than in

the bulk. Our results show that such an assumption is not appropriate; strong electronic coupling

at certain positions at the boundary creates trap states within the band gap of the material. How-

ever, one should also note that electronic coupling between neighboring molecules from opposite

16

sides of the boundary can be weak at certain positions. At these positions, grain boundary acts as a barrier and tends to confine the wave function to one side of the boundary. This effect can be seen from state (10) in Figure 3 and states (3) and (10) in Figure 4. Positions of strong electronic coupling and trap states will be absent only in the case of a grain boundary void when two grains with same orientation are separated by empty space. Consequently, a void (micro-crack) within an organic crystal[54] is expected to act as a barrier.

On the other hand, various numerical simulations of organic crystal FETs were based on a model that considers the transport at the boundary as thermoionic jump over the barrier or tunneling through the barrier.[12,16,21,22] One should note that FETs typically operate at high charge densities. Therefore, the traps become filled with carriers, that in turn create an electrostatic potential that acts as a barrier for the transport of other charges. Such "trap charging induced barriers" should be distinguished from the barriers discussed in the previous paragraph.

Using the obtained results, the density of trap states for naphthalene polycrystals can be estimated. The calculated number of trap states per unit of boundary surface of two misoriented grains is $3 \times 10^{13}\,\mathrm{cm}^{-2}$ in the case of misorientation angle of $5°$ and a-boundary, and takes similar values for other boundaries. Only trapping pairs with mutual distances below $4\,\text{Å}$ were considered in the calculation. In the work of Chwang and Frisbie,[9] the density of trap states was estimated from activation energies for charge transport in a single grain boundary FET based on sexithiophene. It was found that trap densities at acceptor-like levels take values from $7.0 \times 10^{11}\,\mathrm{cm}^{-2}$ to $2.1 \times 10^{13}\,\mathrm{cm}^{-2}$, depending on the grain boundary length and the angle of misorientation. Therefore, our results are of the same order of magnitude as the experimentally based estimate for the material belonging to the same class of materials as naphthalene.

Next, we estimate the number of grain boundary induced trap states per unit of volume and compare it to other relevant material parameters. Typical size of experimentally evidenced monocrystal grains[8,9,20,55] is of the order of $1\,\mu\mathrm{m}$, which translates into volume trap density of $N_\mathrm{t} = 9 \times 10^{17}\,\mathrm{cm}^{-3}$ assuming grains of cubical shape. On the other hand, the number of energy states per unit of volume in the valence band of a bulk naphthalene monocrystal is $N_\mathrm{v} = 6.1 \times 10^{21}\,\mathrm{cm}^{-3}$.

17

Although N_t is much lower than N_v, it can still be significant to affect the charge transport and optical properties of naphthalene. In Ref. 55 grain boundary defects were identified as the most pronounced and the most stable defects. The density of point bulk defects was (over)estimated[55] to be in the $N_p = 10^{14}$-10^{16} cm^{-3} range. Since our calculated value of N_t is larger than N_p, our results confirm the conclusion that grain boundary defects are the most pronounced defects.[55] A compilation of the estimates of the density of trap states from FET characteristics was reported in Ref. 11. The estimated density of states at 0.2 eV above the valence band is in the range $(0.7 - 3) \times 10^{19}$ cm^{-3}eV^{-1}, while at 0.3 eV above the valence band it is in the $(1.5 - 4) \times 10^{18}$ cm^{-3}eV^{-1} (see Fig. 6 in Ref. 11). On the basis of these values one can roughly estimate that the density of trap states with energies higher than 0.2 eV above the valence band to be in the $(10^{17} - 10^{18})$ cm^{-3} range, which is of the same order of magnitude as our calculated N_t.

Finally, we discuss the implications of our findings on properties of electronic and optoelectronic devices based on this class of materials. Since our results show that hole traps are located at the positions of strongest electronic coupling between orbitals of the two molecules from opposite sides of the boundary, one expects that there will be an electronic trap at the same position. We have verified this expectation by performing explicit calculation of electron states at the boundary. As a consequence, traps at grain boundaries will not prevent radiative recombination of electrons and holes in LED devices or light absorption in the case of solar cells. Nevertheless, the traps will certainly broaden the absorption or emission spectrum of the material. Furthermore, the estimated number of traps per unit of volume is comparable to typical charge carrier densities in operating LED and solar cell devices. As a consequence, charge carrier transport will certainly be strongly affected by the traps. On the other hand, FETs typically operate at charge carrier densities much larger than the trap densities. As a consequence, the traps are filled with carriers and affect the charge carrier transport only through electrostatic barriers created by the trapped charges, as discussed previously.

18

Conclusions

In this paper we have introduced the methodology for the calculation of electronic states at grain boundaries in small molecule based organic semiconductors. We focused our study on low-angle grain boundaries, since our results indicated that they have lower energies than high-angle grain boundaries. The results indicate that grain boundaries introduce trap states within the band gap of the material. Wave functions of these states are localized on pairs of molecules from opposite sides of the boundary whose mutual distance is smaller than the distance between two adjacent molecules in a monocrystal. Strong electronic coupling between the orbitals of the two molecules is responsible for the creation of the trap state. While naphthalene molecule was used in our study, we expect that the origin of trap states will be the same in any other small molecule based organic semiconductor since electronic coupling as a mechanism of trap state creation is present in any other material from this class.

The energy of the trap state was found to correlate to the distance between two molecules which create the trap. This correlation was then used to calculate the electronic density of trap states solely based on geometrical arrangement of molecules near the boundary. This approach was exploited to calculate the density of trap states for different boundaries and estimate the number of trap states per unit of volume in a real polycrystal. This number is significant and may consequently reduce the carrier mobility and deteriorate the performance of devices based on polycrystalline organic semiconductors.

Acknowledgments

References

(1) Cheung, D. L.; Troisi, A. Modelling Charge Transport in Organic Semiconductors: From Quantum Dynamics to Soft Matter. *Phys. Chem. Chem. Phys.* **2008**, *10*, 5941–5952.

(2) Friend, R. H.; Gymer, R. W.; Holmes, A. B.; Burroughes, J. H.; Marks, R. N.; et al, Electro-luminescence in Conjugated Polymers. *Nature* **1999**, *397*, 121–128.

(3) Burroughes, J. H.; Bradley, D. D. C.; Brown, A. R.; Marks, R. N.; Mackay, K.; Friend, R. H.; Burns, P. L.; Holmes, A. B. Light-emitting Diodes Based on Conjugated Polymers. *Nature* **1990**, *347*, 539–541.

(4) Colvin, V. L.; Schlamp, M. C.; Alivisatos, A. P. Light-emitting Diodes Made from Cadmium Selenide Nanocrystals and a Semiconducting Polymer. *Nature* **1994**, *370*, 354–357.

(5) Dodabalapur, A.; Torsi, L.; Katz, H. E. Organic Transistors - 2-dimensional Transport and Improved Electrical Characeristics. *Science* **1995**, *268*, 270–271.

(6) Li, G.; Shrotriya, V.; Huang, J. S.; Yao, Y.; Moriarty, T.; Emery, K.; Yang, Y. High-efficiency Solution Processable Polymer Photovoltaic Cells by Self-organization of Polymer Blends. *Nat. Mater.* **2005**, *4*, 864.

(7) Fu, Y.-T.; Risko, C.; Bredás, J.-L. Intermixing at the Pentacene-Fullerene Bilayer Interface: A Molecular Dynamics Study. *Adv. Mater.* **2013**, *25*, 878–882.

(8) Kalihari, V.; Tadmor, E. B.; Haugstad, G.; Frisbie, C. D. Grain Orientation Mapping of Poly-crystalline Organic Semiconductor Films by Transverse Shear Microscopy. *Adv. Mater.* **2008**, *20*, 4033–4039.

(9) Chwang, A. B.; Frisbie, C. D. Temperature and Gate Voltage Dependent Transport Across a Single Organic Semiconductor Grain Boundary. *J. Appl. Phys* **2001**, *90*, 1342–1349.

(10) Chapman, B.; Checco, A.; Pindak, R.; Siegrist, T.; Kloc, C. Dislocations and Grain Boundaries in Semiconducting Rubrene Single-crystals. *J. Cryst. Growth* **2006**, *290*, 479 – 484.

20

(11) Kalb, W. L.; Haas, S.; Krellner, C.; Mathis, T.; Batlogg, B. Trap Density of States in Small-molecule Organic Semiconductors: A Quantitative Comparison of Thin-film Transistors with Single Crystals. *Phys. Rev. B* **2010**, *81*, 155315.

(12) Horowitz, G.; Hajlaoui, M. E. Mobility in Polycrystalline Oligothiophene Field-Effect Transistors Dependent on Grain Size. *Adv. Mater.* **2000**, *12*, 1046–1050.

(13) Nelson, S. F.; Lin, Y.-Y.; Gundlach, D. J.; Jackson, T. N. Temperature-independent Transport in High-mobility Pentacene Transistors. *Appl. Phys. Lett.* **1998**, *72*, 1854–1856.

(14) Sakanoue, T.; Sirringhaus, H. Band-like Temperature Dependence of Mobility in a Solution-processed Organic Semiconductor. *Nat. Mater.* **2010**, *9*, 736–740.

(15) Lee, S. S.; Kim, C. S.; Gomez, E. D.; Purushothaman, B.; Toney, M. F.; Wang, C.; Hexemer, A.; Anthony, J. E.; Loo, Y.-L. Controlling Nucleation and Crystallization in Solution-Processed Organic Semiconductors for Thin-Film Transistors. *Adv. Mater.* **2009**, *21*, 3605–3609.

(16) Chen, J.; Tee, C. K.; Shtein, M.; Anthony, J.; Martin, D. C. Grain-boundary-limited Charge Transport in Solution-processed 6,13 bis(tri-isopropylsilylethynyl) Pentacene Thin Film Transistors. *J. Appl. Phys.* **2008**, *103*, 114513.

(17) Gundlach, D. J.; Royer, J. E.; Park, S. K.; Subramanian, S.; Jurchescu, O. D. Contact-induced Crystallinity for High-performance Soluble Acene-based Transistors and Circuits. *Nat. Mater.* **2008**, *7*, 216–221.

(18) Rivnay, J.; Jimison, L. H.; Northrup, J. E.; Toney, M. F.; Noriega, R.; Lu, S.; Marks, T. J.; Facchetti, A.; Salleo, A. Large Modulation of Carrier Transport by Grain-boundary Molecular Packing and Microstructure in Organic Thin Films. *Nat. Mater.* **2009**, *8*, 952–958.

(19) Dickey, K.; Anthony, J.; Loo, Y.-L. Improving Organic Thin-Film Transistor Performance

through Solvent-Vapor Annealing of Solution-Processable Triethylsilylethynyl Anthradithiophene. *Adv. Mater.* **1976**, *21*, 392.

(20) Carlo, A. D.; Piacenza, F.; Bolognesi, A.; Stadlober, B.; Maresch, H. Influence of Grain Sizes on the Mobility of Organic Thin-film Transistors. *Appl. Phys. Lett.* **2005**, *86*, 263501.

(21) Verlaak, S.; Arkhipov, V.; Heremans, P. Modeling of Transport in Polycrystalline Organic Semiconductor Films. *Appl. Phys. Lett.* **2003**, *82*, 745–747.

(22) Horowitz, G. Tunneling Current in Polycrystalline Organic Thin-Film Transistors. *Adv. Funct. Mater.* **2003**, *13*, 53–60.

(23) Kaake, L. G.; Barbara, P. F.; Zhu, X.-Y. Intrinsic Charge Trapping in Organic and Polymeric Semiconductors: A Physical Chemistry Perspective. *J. Phys. Chem. Lett.* **2010**, *1*, 628–635.

(24) Nan, G.; Li, Z. Modeling of Charge Transport in Polycrystalline Sexithiophene From Quantum Charge Transfer Rate Theory Beyond the First-order Perturbation. *Org. Electron.* **2011**, *12*, 2198 – 2206.

(25) Verlaak, S.; Heremans, P. Molecular Micromolecular View on Electronic States Near Pentacene Grain Boundaries. *Phys. Rev. B* **2007**, *75*, 115127.

(26) Troisi, A.; Orlandi, G. Charge-Transport Regime of Crystalline Organic Semiconductors: Diffusion Limited by Thermal Off-Diagonal Electronic Disorder. *Phys. Rev. Lett.* **2006**, *96*, 086601.

(27) Nan, G.; Yang, X.; Wang, L.; Shuai, Z.; Zhao, Y. Nuclear Tunneling Effects of Charge Transport in Rubrene, Tetracene, and Pentacene. *Phys. Rev. B* **2009**, *79*, 115203.

(28) Shuai, Z.; Wang, L.; Li, Q. Evaluation of Charge Mobility in Organic Materials: From Localized to Delocalized Descriptions at a First-Principles Level. *Adv. Mater.* **2011**, *23*, 1145–1153.
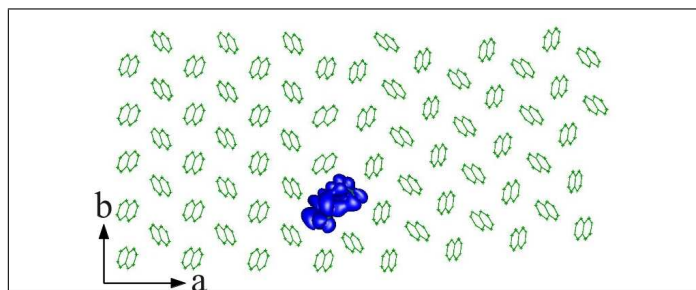
(29) Sánchez-Carrera, R. S.; Atahan, S.; Schrier, J.; Aspuru-Guzik, A. Theoretical Characterization of the Air-Stable, High-Mobility Dinaphtho[2,3-b:2´ 3´-f]thieno[3,2-b]-thiophene Organic Semiconductor. *J. Phys. Chem. C* **2010**, *114*, 2334–2340.

(30) Hannewald, K.; Stojanović, V. M.; Schellekens, J. M. T.; Bobbert, P. A.; Kresse, G.; Hafner, J. Theory of Polaron Bandwidth Narrowing in Organic Molecular Crystals. *Phys. Rev. B* **2004**, *69*, 075211.

(31) Ortmann, F.; Bechstedt, F.; Hannewald, K. Theory of Charge Transport in Organic Crystals: Beyond Holstein's Small-polaron Model. *Phys. Rev. B* **2009**, *79*, 235206.

(32) Martinelli, N. G.; Olivier, Y.; Athanasopoulos, S.; Delgado, M. C. R.; Pigg, K. R.; et al, Influence of Intermolecular Vibrations on the Electronic Coupling in Organic Semiconductors: The Case of Anthracene and Perfluoropentacene. *Chem. Phys. Chem.* **2009**, *10*, 2265–2273.

(33) Ciuchi, S.; Fratini, S. Electronic Transport and Quantum Localization Effects in Organic Semiconductors. *Phys. Rev. B* **2012**, *86*, 245201.

(34) Ciuchi, S.; Fratini, S.; Mayou, D. Transient Localization in Crystalline Organic Semiconductors. *Phys. Rev. B* **2011**, *83*, 081202.

(35) Ciuchi, S.; Fratini, S. Band Dispersion and Electronic Lifetimes in Crystalline Organic Semiconductors. *Phys. Rev. Lett.* **2011**, *106*, 166403.

(36) Perroni, C. A.; Marigliano Ramaglia, V.; Cataudella, V. Effects of Electron Coupling to Intramolecular and Intermolecular Vibrational Modes on the Transport Properties of Single-crystal Organic Semiconductors. *Phys. Rev. B* **2011**, *84*, 014303.

(37) Vukmirović, N.; Bruder, C.; Stojanović, V. M. Electron-Phonon Coupling in Crystalline Organic Semiconductors: Microscopic Evidence for Nonpolaronic Charge Carriers. *Phys. Rev. Lett.* **2012**, *109*, 126407.

(38) Allen, M.; Tildesley, D. J. *Computer Simulation of Liquids*; Clarendon Press, Oxford Science Publications: New York, USA, 1987.

(39) Parr, R. G.; Yang, W. *Density-Functional Theory of Atoms and Molecules*; Oxford University Press: New York, USA, 1989.

(40) Vukmirović, N.; Wang, L. W. Charge Patching Method for Electronic Structure of Organic Systems. *J. Chem. Phys.* **2008**, *128*, 121102.

(41) Vukmirović, N.; Wang, L. W. Electronic Structure of Disordered Conjugated Polymers: Poly-thiophenes. *J. Phys. Chem. B* **2009**, *113*, 409–415.

(42) Martin, M. G.; Siepmann, J. I. Transferable Potentials for Phase Equilibria. 1. United-Atom Description of n-Alkanes. *J. Phys. Chem. B* **1998**, *102*, 2569–2577.

(43) Wick, C. D.; Martin, M. G.; Siepmann, J. I. Transferable Potentials for Phase Equilibria. 4. United-Atom Description of Linear and Branched Alkenes and Alkylbenzenes. *J. Phys Chem. B* **2000**, *104*, 8008–8016.

(44) Rai, N.; Bhatt, D.; Siepmann, J. I.; Fried, L. E. Monte Carlo Simulations of 1,3,5-triamino-2,4,6-trinitrobenzene (TATB): Pressure and Temperature Effects for the Solid Phase and Vapor-liquid Phase Equilibria. *J. Chem. Phys.* **2008**, *129*, 194510.

(45) Rai, N.; Siepmann, J. I. Transferable Potentials for Phase Equilibria. 10. Explicit-Hydrogen Description of Substituted Benzenes and Polycyclic Aromatic Compounds. *J. Phys. Chem. B* **2013**, *117*, 273–288.

(46) Sánchez-Carrera, R. S.; Paramonov, P.; Day, G. M.; Coropceanu, V.; Bredás, J.-L. Interaction of Charge Carriers with Lattice Vibrations in Oligoacene Crystals from Naphthalene to Pentacene. *J. Am. Chem. Soc.* **2010**, *132*, 14437–14446.

(47) Schwoerer, M.; Wolf, H. C. *Organic Molecular Solids*; WILEY-VCH Verlag: Wienheim, Germany, 2008.

24

(48) Hummer, K.; Ambrosch-Draxl, C. Electronic Properties of Oligoacenes from First Principles. *Phys. Rev. B* **2005**, *72*, 205205.

(49) Ponomarev, V. I.; Filipenko, O. S.; Atovmyan, L. O. Improving Organic Thin-Film Transistor Performance through Solvent-Vapor Annealing of Solution-Processable Triethylsilylethynyl Anthradithiophene. *Kristallografiya* **1976**, *21*, 392.

(50) Schmidt, M.; Kusche, R.; Kronmüller, W.; von Issendorff, B.; Haberland, H. Experimental Determination of the Melting Point and Heat Capacity for a Free Cluster of 139 Sodium Atoms. *Phys. Rev. Lett.* **1997**, *79*, 99–102.

(51) Lee, J. A.; Rösner, H.; Corrigan, J. F.; Huang, Y. Phase Transitions of Naphthalene and Its Derivatives Confined in Mesoporous Silicas. *J. Phys. Chem. C* **2011**, *115*, 4738–4748.

(52) Canning, A.; Wang, L. W.; Williamson, A.; Zunger, A. Parallel Empirical Pseudopotential Electronic Structure Calculations for Million Atom Systems. *J. Comp. Phys.* **2000**, *160*, 29 – 41.

(53) Stankovic, I.; Hess, S.; Kröger, M. Structural Changes and Viscoplastic Behavior of a Generic Embedded-atom Model Metal in Steady Shear Flow. *Phys. Rev. E* **2004**, *69*, 021509.

(54) Chen, J.; Tee, C. K.; Yang, J.; Shaw, C.; Shtein, M.; Anthony, J.; Martin, D. C. Thermal and Mechanical Cracking in bis (triisopropylsilylethnyl) Pentacene Thin Films. *J. Polym. Sci. Pt. B-Polym. Phys.* **2006**, *44*, 3631–3641.

(55) Verlaak, S.; Rolin, C.; Heremans, P. Microscopic Description of Elementary Growth Processes and Classification of Structural Defects in Pentacene Thin Films. *J. Phys. Chem. B* **2007**, *111*, 139–150.

(56) This work makes use of results produced by the High-Performance Computing Infrastructure for South East Europe's Research Communities (HP-SEE), a project co-funded by

Graphical TOC Entry

27

Atomic and electronic structure of grain boundaries in crystalline organic semiconductors

Marko Lj. Mladenović, Nenad Vukmirović, Igor Stanković

Scientific Computing Laboratory, Institute of Physics Belgrade, University of Belgrade, Pregrevica 118, 11080 Belgrade, Serbia

E-mail: `markoml@ipb.ac.rs`

Abstract. Grain boundaries in organic crystalline semiconductors play an important role in charge carrier transport. We have developed a method for atomic and electronic structure calculations of grain boundaries in organic semiconductors. Atomic structure is obtained by a Monte Carlo algorithm, while electronic structure is calculated using the charge patching method. The methodology is used to investigate the contact boundary of two naphthalene polycrystals. The existence of the states localized at the boundary is demonstrated and the implications for electronic and optical properties of the materials are discussed.

1. Introduction

Organic semiconductors are very promising materials for electronic and optoelectronics devices, such as transistors, LEDs and solar cells due to their low production cost. Applications of these materials are still limited due to their low carrier mobility and small efficiency. One of the reasons for low carrier mobility in organic crystalline semiconductors is that they form polycrystals and contain many contact interfaces (grain boundaries). The grain boundaries introduce trap states which should act as bottlenecks for charge carrier transport [1]. However, there is very little understanding of the nature of these states, the degree of their localization and their energies.

In this paper, we present a methodology for the investigation of the role of the grain boundaries in polycrystalline organic semiconductors. The methodology is applied to study the localized states at the grain boundaries in polycrystalline naphthalene. The molecular structure of the material near the contact between two grains is obtained as a result of energy minimization by a Monte Carlo (MC) algorithm. The electronic states near the grain boundaries are calculated using the charge patching method (CPM) [2] and the folded spectrum method (FSM) [3]. We present the energies and the wave functions for 10 highest occupied states for naphthalene polycrystals composed of two monocrystals with angles of 5° and 10° between them.
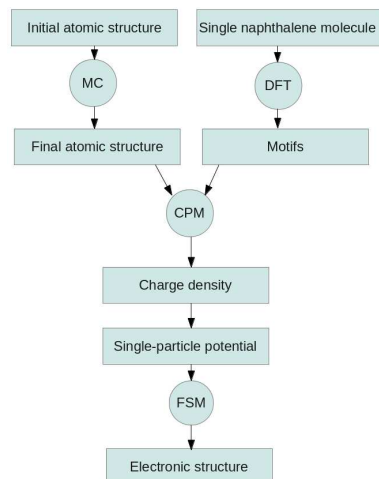
Figure 1. Schematic representation of the algorithm for atomic and electronic structure calculation.

2. The description of the model

Methodology for the calculation of the molecular and electronic structure of grain boundaries in naphthalene polycrystal is described schematically in Figure 1. MC simulations and density functional theory (DFT) calculations are performed separately. They produce equilibrated molecular structure and charge density motifs, respectively, which are the inputs for the electronic structure calculations.

The MC algorithm starts from two ideal naphthalene monocrystals joined together. The interaction between molecules is modeled using Transferable potentials for phase equilibria (TraPPE) [4, 5]. In each step of the MC algorithm a random molecule is translated and rotated for a random vector and angle. This change is accepted or rejected according to the Metropolis algorithm. If the energy of the new configuration is lower than the initial, the change is accepted. Otherwise, the change is accepted with a probability equal to the Boltzmann weight calculated from the difference of the new and the old energy [6]. The simulation is performed until the system reaches thermal equilibrium, i.e. the total potential energy of the system saturates. The MC simulations are performed at 300 K. The obtained configuration is afterwards cooled down to 0 K, also using MC simulations. The cooling rate is chosen so that the ideal crystal structure is recovered far from grain boundary. In this way, possible wave functions localizations induced by dynamic disorder [7] in the atomic structure are excluded.

Charge density motif is a description of the environment of an atom [2]. Two equal atoms can have different motifs if they have different neighboring atoms. There are five motifs in the naphthalene molecule: $C_3 - C_3C_2C_2$, $C_2 - C_3C_2H$, $C_2 - C_2C_2H$, $H - C_2 - C_2C_2$, $H - C_2 - C_3C_2$, where C_X is carbon atom connected to X other carbon atoms.

With the motifs and the atomic structure at hand, one can directly construct the charge density using CPM, avoiding the need for demanding self-consistent solving of
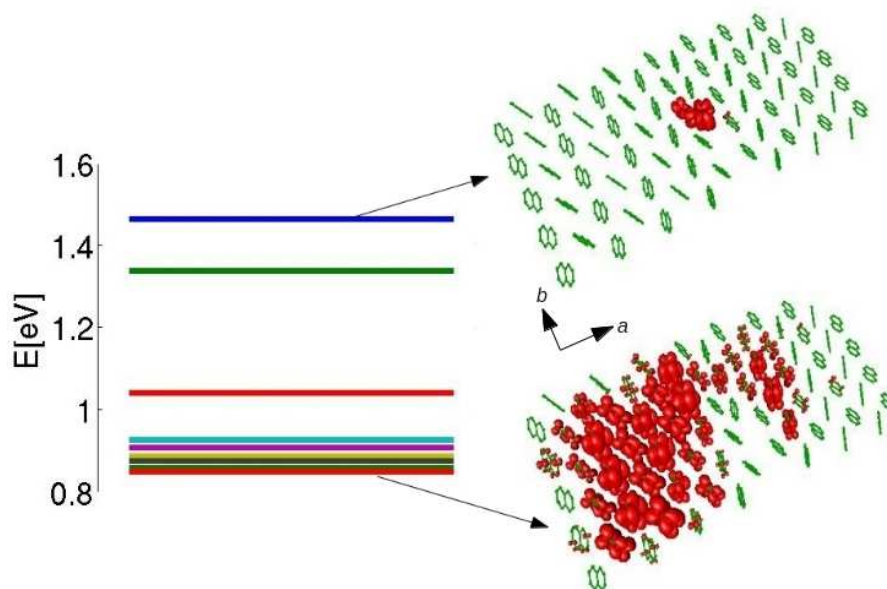
Figure 2. Energies of 10 highest occupied states (left) and wave function isosurface plots of the first (top right) and 10th (bottom right) highest occupied state in the naphthalene polycrystal composed of two monocrystals with the angle of 5° between them. Isosurfaces correspond to the probability of finding a hole inside the surface of 90%.

DFT equations. CPM provides a similar accuracy as DFT but with a much smaller computational cost that allows us to calculate electronic states for systems composed of several thousand atoms, which is not feasible using DFT. When the charge density is obtained, the single-particle Hamiltonian is created by solving the Poisson equation for the single-particle potential. Finally, Schrödinger equation for the single-particle Hamiltonian can be solved using the Folded Spectrum Method [3], that gives the electronic structure (wave functions and energy levels) around the desired energy, which is the top of the valence band in our case.

3. Results and discussion

In this section the obtainted molecular (atomic) and electronic structure of the two naphthalene polycrystals is presented. Molecular structure simulations are performed for a system consisting of 1000 molecules arranged in 10 layers parallel to the ab [8] plane. Electronic structure calculations are performed for a single layer of the polycrystals. This is sufficient to describe the electronic properties of the material, since it is well-known that the electronic coupling in the c direction in naphthalene is much weaker than in the ab plane. We have investigated the grain boundary perpendicular to the a direction of the unit cell of the naphthalene crystal. Results are presented in Figures 2 (angle between the monocrystals is 5°) and 3 (angle between the monocrystals is 10°). On the left hand side of the figures, the energies of 10 highest occupied states are presented. On
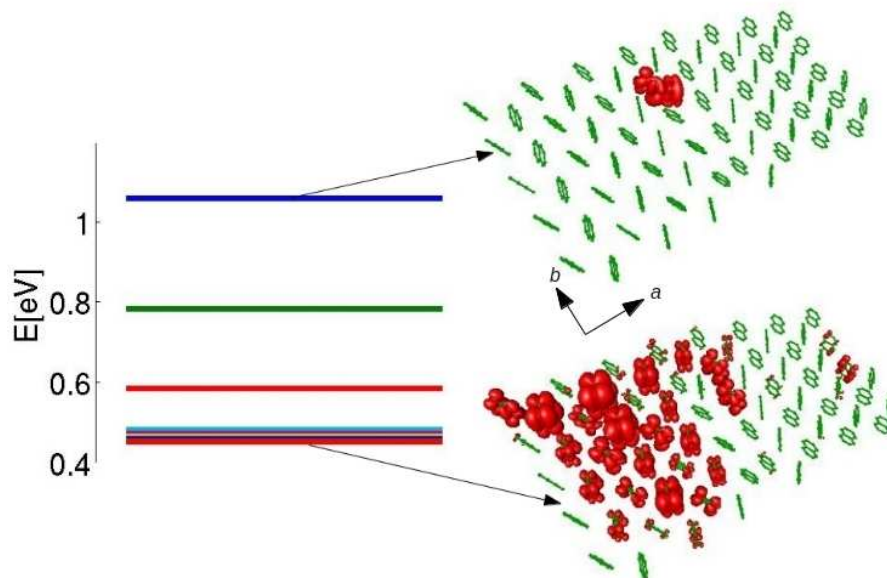
Figure 3. Energies of 10 highest occupied states (left) and wave function isosurface plots of the first (top right) and 10th (bottom right) highest occupied state in the naphthalene polycrystal composed of two monocrystals with the angle of 10° between them. Isosurfaces correspond to the probability of finding a hole inside the surface of 90%.

the right hand side, the atomic structure and the wave functions for the highest (first) and the lowest (10th) calculated states are illustrated.

Our results indicate that the atomic structure of the monocrystal grains stay nearly unchanged if the distance from the grain boundary is greater than half of the dimension of the unit cell in the a direction. Only molecules located at the grain boundary have slightly changed their orientations from the orientations in the monocrystal.

By inspecting the energies of the states of both polycrystals one can notice that there are three states whose energies are significantly higher that the energies of the other states. The highest states are about $0.6\,$eV above the spectral region of delocalized states that originate from monocrystals. For the comparison, the calculated energy gap in the naphthalene monocrystal is about 2.8 eV, which is lower than the experimental band gap $(5.0 - 5.4$ eV [9]) due to the well-known local density approximation (LDA) band gap problem [10]. The highest states are localized on the two molecules belonging to different monocrystals and they are located at the interface between monocrystals. Distance between these two molecules is less than the distance between two neighboring molecules in the monocrystal and consequently electronic coupling of their HOMO orbitals is the largest. On the other hand, the lowest calculated states are completely delocalized, as in the monocrystal. While we have presented the results for only two angles between monocrystals in this work, preliminary calculations for several other angles and boundary surfaces, indicate that the same behavior is generally present.

Charge carrier mobility in the material is expected to strongly depend on the

concentration of trap states, which on the other hand depends on the surface to volume ratio of the crystalline domains and the number of trap states per unit of boundary surface. In devices that operate at low charge carrier concentrations, such as LEDs and solar cell, it may even be possible that all carriers reside in traps in the case of high trap state concentration. In such a case, the presence of traps will strongly reduce the carrier mobility and deteriorate the device performance. On the other hand, in devices that operate at high concentration, such as FETs, one can expect that the traps will be filled by carriers, but the most of the carriers will reside in delocalized states with good transport properties. As a consequence, the impact of trap states on carrier mobility is expected to be less pronounced in FETs compared to LEDs and solar cells.

Finally, we also briefly discuss the impact of trap states on optical properties of this material. In this work, we have shown that hole traps are located at the positions of strongest electronic coupling between orbitals of the two molecules from different monocrystals. One therefore expects that for each electronic trap, there will be a hole trap at the same position. Consequently, such traps will not prevent the radiative recombination of electrons and holes in the case of LEDs or light absorption in the case of solar cells. Nevertheless, the presence of traps will certainly broaden the absorption or emission spectrum of the materials. This may be in some cases undesirable, for example if LEDs with a sharp emission spectrum are required.

4. Conclusions

In this paper, we have introduced the methodology for the atomic and electronic calculations of the grain boundaries in naphthalene polycrystals. Results have shown that grain boundaries have impact on the atomic structure of the polycrystal only in the nearest environment (half of the unit cell) of the boundaries. On the other hand, they produce electronic states which energies are significantly higher than the energies of the delocalized states. Wave functions of these states are located just on the grain boundaries. These states are trap states for the charge carriers and consequently reduce their mobility and deteriorate the performance of devices based on this material.

5. Acknowledgment

6. References

[1] W. L. Kalb, S. Haas, C. Krellner, T. Mathis, and B. Batlogg, Phys. Rev. B **81**, 155315 (2010).
[2] N. Vukmirovic and L.-W. Wang, J. Chem. Phys. **128**, 121102 (2008).

[3] A. Canning, L. Wang, A. Williamson, and A. Zunger, Journal of Computational Physics **160**, 29 (2000).

[4] M. G. Martin and J. I. Siepmann, J. Phys. Chem. B **102**, 2569 (1998).

[5] C. D. Wick, M. G. Martin, and J. I. Siepmann, The Journal of Physical Chemistry B **104**, 8008 (2000).

[6] M. Allen and D.J.Tildesley, *Computer Simulation of Liquids* (Clarendon Press, Oxford Science Publications, 1987).

[7] A. Troisi and G. Orlandi, Phys. Rev. Lett. **96**, 086601 (2006).

[8] M. Schwoerer and H. C. Wolf, *Organic Molecular Solids* (WILEY-VCH Verlag GmbH Co. KGaA, 2008).

[9] K. Hummer and C. Ambrosch-Draxl, Phys. Rev. B **72**, 205205 (2005).

[10] A. Seidl, A. Görling, P. Vogl, J. A. Majewski, and M. Levy, Phys. Rev. B **53**, 3764 (1996).

Monte Carlo Simulations of
Crystalline Organic Semiconductors

Marko Mladenović[1], Igor Stanković[1]

Abstract: Molecular model for crystalline organic semiconductors based on small molecules is implemented in three-dimensional Monte Carlo simulations. In this paper results for naphthalene are presented. Molecular structure is considered in two configurations: within a single monocrystal and in vicinity of interface between two monocrystals with different crystalline orientations.

Keywords: Organic semiconductors, Monte Carlo algorithm, Polycrystal.

1   Introduction

Idea of using organic materials as active elements for electronic devices was proposed only a few years after the first classical silicon-based electronic device had been made [1 – 3]. Research on organic semiconductors has been intensified during 90s for two reasons: (1) experiments proved that it was possible to make organic lights emitting diodes (OLED) [1, 4 – 7], organic thin film transistors (OTFT) [1, 8] and organic solar cells (OPV) [1, 9]; (2) at the same time new cheap semiconducting devices were required. At this moment, organic LEDs are on the market, but OTFTs and OPVs are still subject of research effort, which includes development of new materials, processing techniques and devices architectures [1].

Organic semiconductors can be either polymer or based on small molecules. The organic semiconductors with small molecules exist both in amorphous and crystalline state. Small molecules used in the organic semiconductors are frequently aromatic hydrocarbons such as naphthalene, anthracene, pentacene, rubrene etc. PPV, P3HT are examples of polymer semiconductors. In this paper simulations of naphthalene are presented.

Organic thin film based on the naphthalene crystal is typically polycrystalline, which means that inside one polycrystalline film there are many contact interfaces (grain boundaries) between different monocrystals with different crystalline orientations. Grain boundaries are believed to be a

---

[1]Institute of Physics Belgrade, University of Belgrade, Pregrevica 118, 11080 Zemun, Serbia
 E-mails: markoml@ipb.ac.rs, igor@ipb.ac.rs

bottleneck for charge carrier transport in organic semiconductors. Exact physics of the transport at grain boundaries is still not known.

The goal of this work is modeling of the structure of a grain boundary between two naphthalene monocrystals with a given angle of disorientation. For this purpose, simulations based on well-known classical Monte Carlo (MC) method were developed. Until now, Monte Carlo method has been widely used for quantum mechanical simulations of organic semiconductors, mostly for charge transport modeling. Yao and co-workers have applied MC method to determine waiting time and diffusion coefficient of carriers in pentacene [10]. Further, Monte Carlo-based transport simulator has been developed to calculate field and temperature dependent mobility in thiophene- and porphyrin-based OTFTs [11]. Dynamical MC has been used to obtain the dependence of internal quantum efficiency of an organic bulk heterojunction PFB/F8BT solar cell [12]. In this paper, classical molecular MC is used for the first time to investigate the role of grain boundaries in naphtahlene. In Section 2 the methodology is described, while results of the simulation of a bulk naphthalene monocrystal and the structure around the grain boundary of two monocrystals are presented in Section 3.

2   Method Description

The crystal structure of naphthalene is illustrated in Fig. 1. The unit cell of naphthalene crystal is monoclinic [10] (two pairs of unit vectors are perpendicular) and contains 2 molecules with angle between them of 51.9°. The Lennard–Jones potential is used to describe interaction between molecules and the Monte Carlo method to obtain the structure at finite temperature.
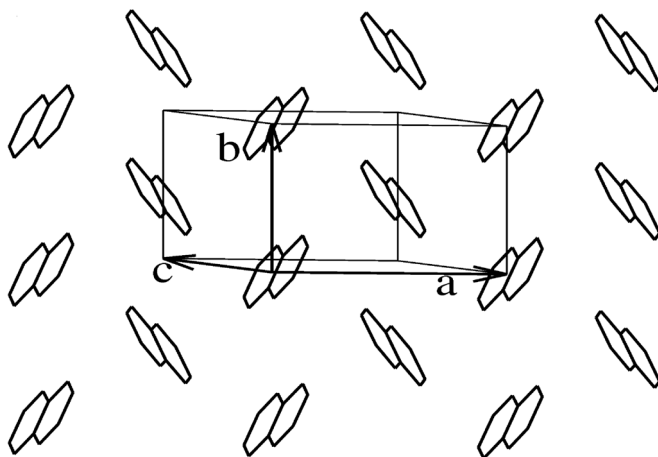

Fig. 1 – *The crystal structure of naphthalene. Dimensions of the unit cell are*: a = 0.824 nm, b = 0.6 nm and c = 0.866 nm [10].

2.1 Lennard – Jones Potential

Interaction between molecules is described using Lennard – Jones potential, which is given by formula:

$$v^{LJ}(r) = 4\varepsilon \left(\left(\frac{\sigma}{r} \right)^{12} - \left(\frac{\sigma}{r} \right)^{6} \right), \tag{1}$$

where r is a distance between CH groups from different molecules. When calculating the total energy of the simulated system, only interactions of CH groups from different molecules are considered. The shape of the potential is illustrated in Fig. 2.
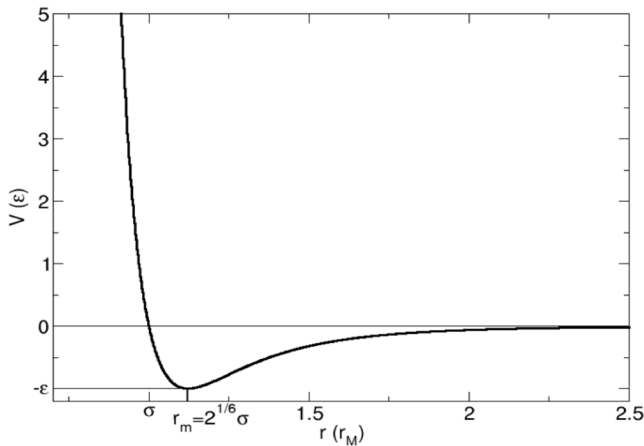
Fig. 2 – *Lennard Jones Potential.*

Here, ε is absolute value of potential at the minimum and it is called potential depth. Parameter σ is distance between atom groups at which the interaction potential is 0. As we can see in Fig. 2, potential for distances greater than 2σ is very small compared to molecule kinetic energy at the room temperature. Here, it is convenient to introduce cut-off parameter for the potential at 4σ. In such a way, simulation becomes faster without lower certainty of the results. In our simulations, scaled Lennard Jones Potential is used ($\varepsilon = \sigma = 1$). Therefore all variables should be scaled using scaled units: (1) distance $d^* = \sigma = 0.37$nm, (2) density $\rho^* = 1/\sigma^3 = 20$ nm^{-3} and (3) temperature $T^* = \varepsilon/k_B = 50$ K [14, 15].

2.2 Monte Carlo Method

Monte Carlo Algorithm is schematically described in Fig. 3. Molecules are considered as rigid and in-plane, therefore their shape and bonding lengths between atoms are constant during the simulation. The center of mass of a molecule has 6 degrees of freedom: 3 translational and 3 angles which describe

rotation. We use Tait-Bryan angles, which represent one of the Euler angles conventions. The algorithm starts from a given or a random configuration of molecules [16]. Two types of predefined configurations are possible: (1) mono-crystaline and (2) interface. In the case of interface, the initial configuration is created from two monocrystals joined together with a defined angle between them. After an initial configuration is created, two nested cycles start. The first cycle is repeated M times, where M is given number of MC steps, and the second is repeated N times, where N is number of molecules in the system. In each MC step the energy of the system E_{int} is calculated. Then, one molecule is randomly chosen, translated and rotated. In total, during the MC simulations maximal $N \times M$ random moves of randomly chosen molecules are tried. After each change of the configuration, energy of the new configuration of E_{new} is calculated. The change is accepted or not according to the Metropolis condition: if new energy is lower than the initial, new configuration is accepted, if it is not, than it is accepted with a probability equal to the Boltzmann weight of the difference of the new and the initial energy, i.e., $\exp[-(E_{new}-E_{init})/k_BT]$ see [16, 17]. The Monte Carlo simulation reaches thermal equilibrium when the total potential energy of the system start to oscillate around a fixed value. An evolution of the total potential energy during MC run is shown in Fig. 4 for a typical simulation performed at 300 K. The obtained configuration is afterwards cooled down to 0 K, also using MC simulation. The cooling rate is chosen so that the equilibrium crystal structure is recovered.
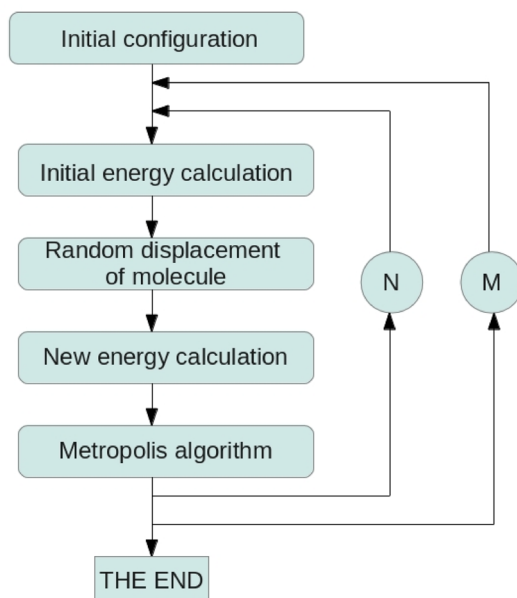
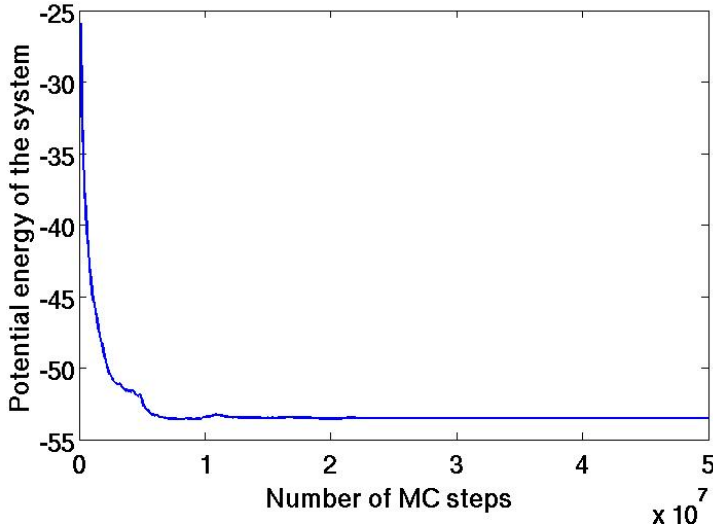

Fig. 3 – *The Monte Carlo algorithm.*

Fig. 4 – *Evolution of the potential energy of the system with N = 1000 naphthalene molecules.*

2.3 Order parameter

In order to monitor level of the orientational order in the obtained structure we use the order parameter [18]. The order parameter is defined by the vector, called director, which is directed through the reference axis of a molecule. Orientation of the molecule is described by two angles φ and θ. The components of director are given by equations:

$$\vec{u}_x = \cos\varphi \sin\theta , \qquad (2)$$

$$\vec{u}_y = \sin\varphi \sin\theta , \qquad (3)$$

$$\vec{u}_z = \cos\theta . \qquad (4)$$

Using this components the matrix is formed:

$$Q_{\alpha\beta} = \frac{1}{2N} \sum_i (\vec{u}_{\alpha i} \vec{u}_{\beta i} - \delta_{\alpha\beta}) , \qquad (5)$$

where is N number of molecules, α and β are combination of x, y, z axes and $\delta_{\alpha\beta}$ is the Kronicker function [18]. Diagonalization of the matrix gives 3 eigenvalues. Maximal eigenvalue is the order parameter. It has values from 0 to 1. Crystal structure has the order parameter close to 1, liquid crystal between 0.1 and 0.4 and isotropic system under 0.1 [18].

3 Results

3.1 Simulations of naphthalene monocrystal

For the algorithm correctness checkout, the naphthalene bulk monocrystal is simulated. During the simulation, number of molecules, temperature and volume are kept constant (NVT ensemble). System consists of 1000 molecules arranged in 10 layers parallel to the *ab* plane. In Fig. 5, the potential energy and the order parameter dependence on temperature are given. Temperature rises from 0 K to the just below melting temperature of 350 K. The potential energy increases and the order parameter decreases with the temperature increase. Still, since the material maintains its crystal structure both magnitudes of the potential energy (compared to molecular kinetic energy) and order parameter remain high.
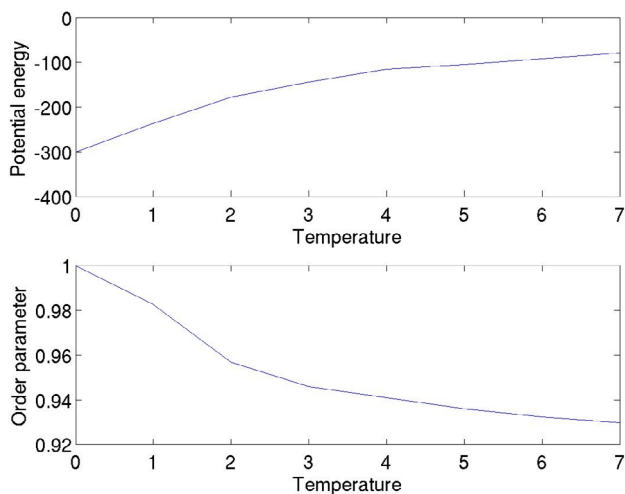
Fig. 5 – a) *Potential energy dependence and*
b) *order parameter dependence on temperature.*
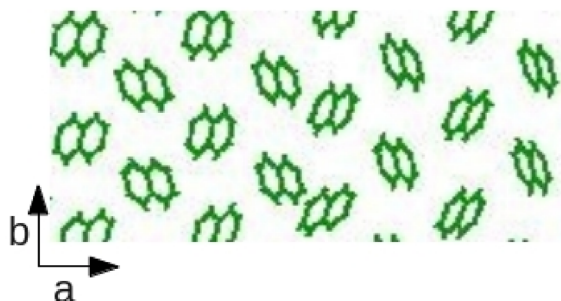*All variables are expressed in non-dimensional Lennard-Jones units.*

Fig. 6a – *The molecular structure over naphthalene*
polycrystal for angle between monocrystal of 5°.
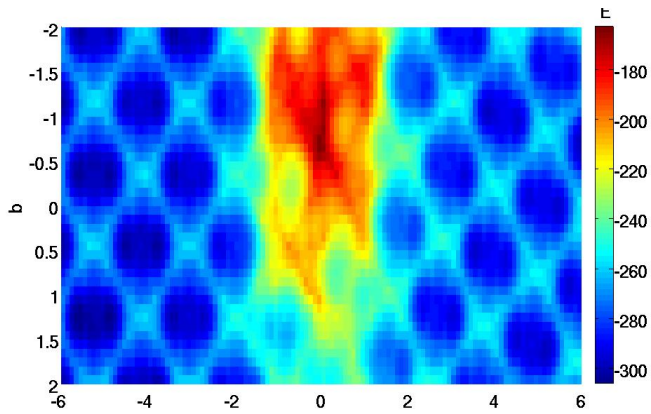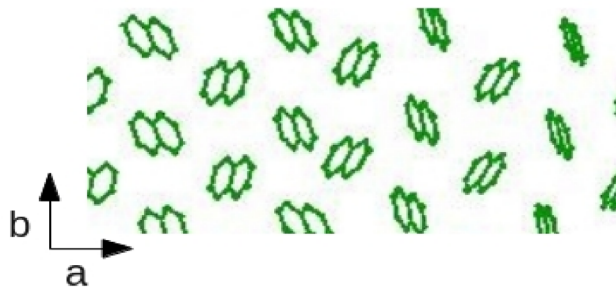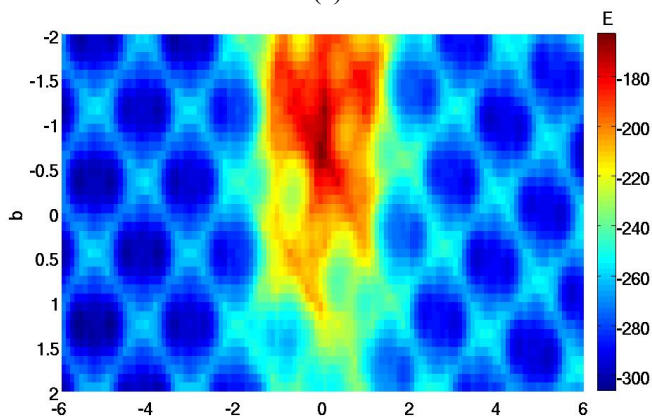*All variables are expressed in non – dimensional Lennard Jones units.*

Fig. 6b – *Energy distribution over naphthalene polycrystal for angle between monocrystal of* 5°. *All variables are expressed in non – dimensional Lennard Jones units.*

(a)

(b)

Fig. 7 – *The molecular structure* (a) *and energy distribution* (b) *over naphthalene polycrystal for angle between monocrystal of* 10°. *All variables are expressed in non – dimensional Lennard Jones units.*

3.2 Simulations of grain boundaries between two monocrystals

In this section, results of simulations of grain boundaries in naphthalene polycrystal are presented. The interface is created by joining two monocrystals with different crystalline orientations. The number of molecules is 500 in each monocrystal. The grain boundary is perpendicular to *a* direction of the unit cell of the naphthalene crystal. Our results indicate that the molecular structure of the monocrystal grains is changed only in the vicinity of the grain boundary. Fig. 6 and Fig. 7 show the molecular structure of grain boundaries as well as the energy distribution over one *ab* plane for angles between monocrystals of 5º and 10º. The highest energies are concentrated on the grain boundary. In Fig. 8 potential energy dependence on the angle between monocrystals is given. The energy increases as angle increases.
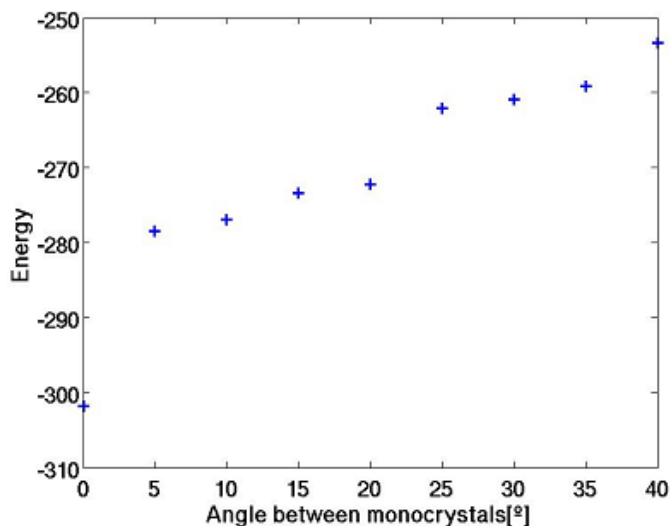

Fig. 8 – *The potential energy of a polycrystal dependence on angle between monocrystals. Energy is expressed in non – dimensional Lennard Jones units.*

4   Conclusion

In this paper, three-dimensional Monte Carlo simulations are presented, in which the molecular model for crystalline organic semiconductors based on the naphthalene is implemented. The dependence of potential energy and order parameter on temperature in the crystalline naphthalene are evaluated. The results for the bulk naphthalene monocrystal and for the grain boundaries in the naphthalene polycrystal are shown. The results for naphthalene polycrystal

indicate that grain boundaries have impact on the molecular structure of the polycrystal only in the nearest environment of the boundaries. Molecules near the boundary have significantly higher energies than molecules far from the boundary. Also, their orientation is different from the orientation of molecules in monocrystal grains. Obtained results for the molecular structure of grain boundaries in naphthalene polycrystals will be used for electronic calculations which should give answer how do grain boundaries affect transport properties of crystalline organic semiconductors based on small molecules.

5 Acknowledgment

6 References

[1]   D.L. Cheung, A.Troisi: Modelling Charge Transport in Organic Semiconductors: From Quantum Dynamics to Soft Matter, Physical Chemistry Chemical Physics, Vol. 10, No. 39, Aug. 2008, pp. 5941 – 5952.

[2]   M. Berggen, D. Nilsson, N.D. Robinson: Organic Materials for Printed Electronics, Nature Materials, Vol. 6, No. 1, Jan. 2007, pp. 3 – 5.

[3]   S. R. Forrest: The Path to Ubiquitous and Low-cost Organic Electronic Appliances on Plastic, Nature, Vol. 428, No. 6986, April 2004, pp. 911 – 918.

[4]   R.H. Friend, R.W. Gymer, A.B. Holmes, J.H. Burroughes, R.N. Marks, C. Taliani, D.D.C. Bradley, D.A.D. Santos, J.L. Bredas, M. Logdlund, W.R. Salaneck: Electroluminescence in Conjugated Polymers, Nature, Vol. 397, No. 6715, Jan. 1999, pp. 121 – 128.

[5]   J.H. Burroughes, D.D.C. Bradley, A.R. Brown, R.N. Marks, K. Mackay, R.H. Friend, P.L. Burns, A.B. Holms: Light-emitting Diodes based on Conjugated Polymers, Nature, Vol. 347, No. 6293, Oct. 1990, 347, pp. 539 – 541.

[6]   V.L. Colvin, M.C. Schlamp, A.P. Alivisatos: Light-emitting Diodes Made from Cadmium Selenide Nanocrystals and a Semiconducting Polymer, Nature, Vol. 370, No. 6488, Aug. 1994, pp. 354 – 357.

[7]   W.L. Kalb, S. Haas, C. Krellner, T. Mathis, B. Batlogg: Trap Density of States in Small-molecule Organic Semiconductors: A Quantitative Comparison of Thin-film Transistors

with Single Crystals, Physical Review B: Condensed Matter and Materials Physics, Vol. 81, No. 15, April 2010, p. 155315.

[8] G. Li, V. Shrotriya, J.S. Huang, Y. Yao, T. Morairty, K. Emery, Y. Yang: High-efficiency Solution Processable Polymer Photovoltaic Cells by Self-organization of Polymer Blends, Nature Materials, Vol. 4, No. 11, Nov. 2005, pp. 864 – 868.

[9] A. Dodabalapur, L. Trosi, H. E. Katz: Organic Transistors: Two-dimensional Transport and Improved Electrical Characteristics, Science, Vol. 268, No. 5208, April 1995, pp. 270 – 271.

[10] M. Grundndmann: The Physics of Semiconductors: An Introduction Including Nanophysics and Applications, Springer, Berlin, Germany, 2010.

[11] Y. Yao, W. Si, X. Hou, C. Q. Wu: Monte Carlo Ssimulation based on Dynamic Disorder Model in Organic Semiconductors: From Coherent to Incoherent Transport, Journal of Chemical Physics, Vol. 136, No. 23, June 2012, p. 234106.

[12] A. Bolognesi, A. Di Carlo, P. Lugli, G. Conte: Large Drift-diffusion and Monte Carlo Modeling of Organic Semiconductor Devices, Synthetic Metals, Vol. 138, No. 1-2, June 2003, pp. 95 – 100.

[13] P.K. Watkins, A.B. Walker, G.L.B. Verscfoor: Dynamical Monte Carlo Modelling of Organic Solar Cells: The Dependence of Internal Quantum Efficiency on Morphology, Nano Letters, Vol. 5, No. 9, Aug. 2005, pp. 1814 – 1818.

[14] C.D. Wick, M.G. Martin, J.I. Siepmann: Transferable Potentials for Phase Equilibria. 4. United-Atom Description of Linear and Branched Alkenes and Alkylbenzenes, The Journal of Physical Chemistry B, Vol. 104, No. 33, Aug. 2000, pp. 8008 – 8016.

[15] M.G. Martin, J.I. Siepmann: Transferable Potentials for Phase Equilibria. 1. United-atom Description of n-Alkanes, The Journal of Physical Chemistry B, Vol. 102, No. 14, April 1998, pp. 2569 – 2577.

[16] M.P. Allen, D.J. Tildesey: Computer Simulations of Liquids, Oxford University Press, NY, USA, 1999.

[17] D. Frenkel, B. Smit: Understanding Molecular Simulations: From Algorithms to Applications, Academic Press, San Diego, CA, USA, 2002.

[18] H. Steuer: Thermodynamical Properties of a Model Liquid Crystal, PhD Thesis, Technical University Berlin, Berlin, Germany, 2004.

Република Србија
Универзитет у Београду
Електротехнички факултет
Д.Бр.2012/5021
Датум: 30.11.2012. године

На основу члана 161 Закона о општем управном поступку и службене евиденције издаје се

УВЕРЕЊЕ

Младеновић (Љубиша) Марко, бр. индекса 2012/5021, рођен 02.09.1988. године, Зајечар, Република Србија, уписан школске 2012/2013. године, у статусу: финансирање из буџета; тип студија: докторске академске студије; студијски програм: Електротехника и рачунарство, модул Наноелектроника и фотоника.

Према Статуту факултета студије трају (број година): три студијске године и има најмање 180 ЕСПБ бодова.

Рок за завршетак студија: у двоструком трајању студија.

Ово се уверење може употребити за регулисање војне обавезе, издавање визе, права на дечији додатак, породичне пензије, инвалидског додатка, добијања   здравствене књижице, легитимације за повлашћену вожњу и стипендије.

Овлашћено лице факултета

На основу члана 161 Закона о општем управном поступку ("Службени лист СРЈ", бр. 33/97, 31/2001 и "Службени гласник РС", бр. 30/2010), дозволе за рад број 612-00-588/2008-04 од 17.11.2008. године коју је издало Министарство просвете Републике Србије и службене евиденције, Универзитет у Београду - Електротехнички факултет, издаје

УВЕРЕЊЕ

Марко Младеновић

име једног родитеља Љубиша, ЈМБГ 0209988750049, рођен 02.09.1988. године, Зајечар, Република Србија, уписан школске 2007/08. године, дана 15.09.2011. године завршио је основне академске студије на студијском програму Електротехника и рачунарство, модул Физичка електроника - смер Наноелектроника, оптоелектроника и ласерска техника, у трајању од четири године, обима 240 (две стотине четрдесет) ЕСПБ бодова, са просечном оценом 9,78 (девет и 78/ 100).

На основу наведеног издаје му се ово уверење о стеченом високом образовању и стручном називу **дипломирани инжењер електротехнике и рачунарства**.

Декан

Проф. др Миодраг Поповић

На основу члана 161 Закона о општем управном поступку ("Службени лист СРЈ", бр. 33/97, 31/2001 и "Службени гласник РС", бр. 30/2010), дозволе за рад број 612-00-588/2008-04 од 17.11.2008. године коју је издало Министарство просвете Републике Србије и службене евиденције, Универзитет у Београду - Електротехнички факултет, издаје

УВЕРЕЊЕ

Марко Младеновић

име једног родитеља Љубиша, ЈМБГ 0209988750049, рођен 02.09.1988. године, Зајечар, Република Србија, уписан школске 2011/12. године, дана 17.09.2012. године завршио је мастер академске студије на студијском програму Електротехника и рачунарство, модул Наноелектроника, оптоелектроника и ласерска техника, у трајању од једне године, обима 60 (шездесет) ЕСПБ бодова, са просечном оценом 10,00 (десет и 00/100).

На основу наведеног издаје му се ово уверење о стеченом високом образовању и академском називу **мастер инжењер електротехнике и рачунарства.**

Декан

Проф. др Миодраг Поповић